Analyzing the Hydroclimatic Teleconnections of Summer Monsoon Rainfall in Kerala, India, Using Multivariate Empirical Mode Decomposition and Time-Dependent Intrinsic Correlation

Adarsh Sankaran and Manne Janga Reddy

***Abstract*—This letter presents an alternative approach for investigating the teleconnections of summer monsoon rainfall in the state of Kerala, India, with four prominent climatic oscillations in multiple time scales based on multivariate empirical mode decomposition (EMD) (MEMD) and time-dependent intrinsic correlation (TDIC). First, the multivariate data set constituting summer monsoon rainfall time series and the climate oscillations such as the Quasi-Biennial Oscillation, El Niño Southern Oscillation (ENSO), Atlantic Multidecadal Oscillation, and Equatorial Indian Ocean Oscillation are decomposed to several rotational modes by employing MEMD. To capture the associations in shorter time spells, the TDIC method is employed, in which the sliding window is adaptively fixed based on instantaneous periods obtained by the Hilbert transform of the obtained modes. From the analysis, it is found that the strength and nature of association between summer monsoon rainfall and the climate oscillations vary with time scales and time spells. The performance of MEMD-based TDIC analysis is compared with that of EMD-based TDIC, and it was found that the former one well captured the direct correlation between ENSO and summer monsoon rainfall in the 1997–1998 period and the opposing correlation in the 2002–2003 period, while the latter approach failed to capture such associations properly.**

***Index Terms*—Correlation, multivariate empirical mode decomposition (EMD) (MEMD), monsoon, oscillations, rainfall, time-dependent intrinsic correlation (TDIC).**

I. INTRODUCTION

THE characterization and forecasting of the Indian summer monsoon rainfall has received wide attention by meteorologists and hydrologists. In the past, many attempts have been made to understand the teleconnection between the Indian summer monsoon rainfall and different climatic oscillations [1]–[5]. Also, many studies highlighted the importance of performing such teleconnection studies at smaller geographical scales such as subdivisions for the accurate predictions of local scale hydrological variables [6]–[9]. The empirical mode decomposition (EMD) proposed by Huang *et al.* [10] is a data-adaptive multiscale decomposition method, which decomposes a time series signal into different oscillatory modes called intrinsic mode functions (IMFs), each of which governs some physical processes with specific periodicity. The obtained IMFs are the most appropriate inputs to perform the Hilbert transform (HT), which may help to study the spectral characteristics of a nonlinear and nonstationary time series in the time-frequency domain, by finding the instantaneous frequencies and amplitudes. The spectral analysis technique which combines EMD and HT is called as the Hilbert–Huang transform (HHT). The HHT-based running correlation analysis technique, namely, the time-dependent intrinsic correlation (TDIC) proposed by Chen *et al.* [11], is a useful means to investigate the link between two nonlinear and nonstationary time series signals at shorter time spells [12], [13]. Even though EMD and its variants are widely used for the analysis of geoscience data sets, it sometimes shows mode misalignment, i.e., it may not result in the same number of IMFs for all components of multivariate data sets, which often creates problems in teleconnection studies employing the TDIC. Rehman and Mandic [14] proposed a multivariate extension of EMD, which has the ability to align common scales present within multivariate data. Each "common scale" is manifested in the common oscillatory modes in all the variates within an m-variate data set. Such "mode alignment" property helps to make use of similar scales in different data sets, and thus, the obtained scales represent the "true" scales of underlying processes. Furthermore, multivariate EMD (MEMD) represents a more powerful filter bank and reduces mode mixing compared with the EMD or its variants such as the ensemble EMD [15].

In this letter, the MEMD–TDIC coupled approach is presented as an effective tool to investigate the hydroclimatic teleconnections. Here, the summer monsoon rainfall time series from the Kerala meteorological subdivision in India, along with four different climate oscillations such as Quasi-Biennial Oscillation (QBO), El Niño Southern Oscillation (ENSO), Atlantic Multidecadal Oscillation (AMO), and Equatorial Indian Ocean Oscillation (EQUINOO), constitute the multivariate data set. The rest of this letter is organized as follows. First, a brief overview of different techniques adopted in this letter is presented in Section II. The details of the study area and data used are given in Section III. The application of the MEMD–TDIC approach and the obtained results are presented in Section IV.

Manuscript received January 12, 2016; revised May 10, 2016; accepted May 30, 2016. Date of publication June 23, 2016; date of current version August 5, 2016.

A. Sankaran is with the Indian Institute of Technology Bombay, Mumbai 400 076, India, and also with the Thangal Kunju Musaliar College of Engineering Kollam, Kollam 691 005, India (e-mail: adarsh_lce@yahoo.co.in).

M. Janga Reddy is with the Indian Institute of Technology Bombay, Mumbai 400 076, India (e-mail: mjreddy@civil.iitb.ac.in).

Color versions of one or more of the figures in this paper are available online at http://ieeexplore.ieee.org.

Digital Object Identifier 10.1109/LGRS.2016.2577598

A discussion on the efficacy of the proposed approach is presented in Section V. The conclusions drawn from this letter are summarized in Section VI.

II. Methodology

In general, the procedure for investigating hydroclimatic teleconnections between summer monsoon rainfall and climatic variables in multiple time scales involves the following: 1) decomposing each time series into low and high frequency modes using an appropriate decomposition technique and 2) performing a correlation analysis between the corresponding modes at different process scales. The main steps involved in the proposed approach of this letter are as follows.

1) Decompose multivariate data sets using MEMD.
2) Apply normalized HT (NHT) with direct quadrature (DQ) (NHT-DQ) [16] to find the instantaneous frequency (and hence the instantaneous period).
3) Employ the TDIC method to perform the multiscale running correlation between corresponding IMFs of the rainfall and climate oscillations.

A. MEMD

MEMD [14] decomposes multiple time series simultaneously after identifying the common scales inherent in the different time series of concern. A brief description of the MEMD algorithm is presented here [14], [15], [17].

In this method, multiple envelops are produced by taking projections of the multiple inputs along different directions in an m-dimensional space.

Assuming that $V(t) = \{v_1(t), v_2(t), \ldots, v_m(t)\}$ denotes the m vectors as a function of time t and $X^{\theta_k} = \{x_1^k, x_2^k, \ldots, x_m^k\}$ denotes the direction vector along different directions given by angles $\theta_k = \{\theta_1^k, \theta_2^k, \ldots, \theta_{m-1}^k\}$ in a direction set X ($k = 1, 2, 3, \ldots, K$; K is the total number of directions). It can be noted that the rotational modes appear as the counterparts of the oscillatory modes in EMD or its variants. The IMFs of m temporal data sets can be obtained by the following algorithm.

1) Generate a suitable set of direction vectors by sampling on a $(m-1)$ unit hypersphere.
2) Calculate the projection $p^{\theta_k}(t)$ of the data sets $V(t)$ along the direction vector X^{θ_k} for all k.
3) Find temporal instants $t_i^{\theta_k}$ corresponding to the maxima of projection for all k.
4) Interpolate $[t_i^{\theta_k}, V(t_i^{\theta_k})]$ to obtain multivariate envelop curves $e^{\theta_k(t)}$ for all k.
5) The mean of envelope curves $(M(t))$ is calculated by $M(t) = (1/K)\sum_{k=1}^{K} e^{\theta_k(t)}$.
6) Extract the "detail" $D(t)$ using $D(t) = V(t) - M(t)$. If $D(t)$ fulfills the stoppage criterion for a multivariate IMF, apply the aforementioned procedure to $V(t) - D(t)$; otherwise, apply it to $D(t)$.

For the generation of direction vectors, the Hammersley sampling sequence can be used [15], and the stopping criteria proposed by Huang *et al.* [18] can be used in the implementation of MEMD.

B. NHT-DQ

The Hilbert transformation of IMFs obtained by MEMD gives instantaneous frequencies and amplitudes to study the spectral properties of the time series. To avoid the chances of getting negative instantaneous frequencies (which are physically meaningless) and to ensure the mathematical correctness of the transformation [19], [20], Huang *et al.* [16] proposed a normalization scheme for HT. The normalization scheme primarily involves the following: 1) the identification of local maxima of IMFs; 2) spline fitting through maxima points; and 3) term-by-term division of IMFs by the constructed spline, etc. The third step is repeated iteratively until the normalized maximum values are all unity. The final series will be the frequency-modulated part from which the amplitude modulated (AM) part of the signal is extracted. The combination of this normalization process and application of the HT to the AM signal is called the NHT method, and the use of "*arccosine*" instead of "*arctan*" in the computation of phase angles makes the scheme "DQ" [16]. In this letter, the NHT-DQ scheme is used to find the instantaneous frequencies required to perform the TDIC analysis.

C. TDIC

Chen *et al.* [11] proposed a method, namely, TDIC, for determining scale-dependent correlation between two time series. This method employs the following steps.

1) Decompose both the time series data of concern into multiple time scales using EMD (or its variants).
2) Perform HT of the different modes, and extract the instantaneous frequency (and hence the instantaneous period) from them.
3) Select $t_w \geq t_d$, and define the local interval centered around t as $I_{t_w}(t) = [t - (t_w/2), t + (t_w/2)]$ where $t_d = \max(T_{1,i}, T_{2,i})$ where and are instantaneous periods of the ith mode of time series 1 and 2, respectively.
4) Compute the local correlation between the two IMFs as $R_{t_w}(t) = corr(\mathrm{IMF}_{1,i}(t), \mathrm{IMF}_{2,i}(t))$ for the segment of the series having length $I_{t_w}(t)$.
5) Perform Student's t-test to investigate the significance of local correlations.
6) Repeat steps 3 to 5 iteratively until the boundary of the sliding window exceeds the end points of the time series.

After computing the correlation for different sliding windows, the TDIC plot is prepared. The horizontal axis of the TDIC plot is the time (which corresponds to the center position of the sliding window), and the vertical axis is the size of the sliding window. In general, half of the data length is selected as the maximum size of the sliding window, and more details on the algorithm can be found elsewhere [11], [12].

III. Study Area and Data Sets

In this letter, the monthly rainfall data of the Kerala meteorological subdivision (8.5° N, 76.98° E) in India is selected for the demonstration of the proposed approach. The Kerala state is located in the western coast of Southern India, and it is popularly known as the "gateway of the Indian monsoon." The annual average rainfall of Kerala is quite high (∼300 cm) when compared with that of the country (∼120 cm). Here, the summer monsoon season (June–July–August–September) is the prominent rainfall season in which the state receives more than 60% of the annual rainfall. The monthly summer monsoon rainfall data for the period 1950–2012 were collected from the Indian Institute of Tropical Meteorology Pune, and the data of four different climate oscillations were collected from different organizations. The monthly data of QBO was obtained from the website of the National Oceanic and Atmospheric Administration (NOAA) Earth System Research Laboratory for the period 1950–2012. The intensities of El Niño events are generally assessed on the basis of the average sea surface temperature (SST) over different Niño regions in the Pacific Ocean within specific latitudes and longitudes. From past studies, it was noted that summer monsoon rainfall over different parts of India, including Kerala, is best associated with the SST anomaly from the Niño 3.4 region [3], [9], [21], [22]. The data of the SST anomaly corresponding to the Niño 3.4 region (120° W–170° W, 5° S–5° N) called as the Oceanic Niño Index were obtained from NOAA National Weather Service Climate Prediction Center for the period 1950–2012 and used as the ENSO index. The data of monthly AMO indices were obtained from the NOAA National Weather Service Climate Prediction Center for the period 1950–2012. The data of the zonal wind component for the region (60–90° E, 2.5° S–2.5° N) were obtained from the National Centers for Environmental Prediction for the same period. The EQUINOO index was defined as the negative of the anomaly of the zonal component of surface wind in the equatorial Indian Ocean region (60–90° E, 2.5° S–2.5° N).

IV. Investigating Hydroclimatic Teleconnection Using MEMD–TDIC Approach

The "hydroclimatic teleconnection" refers to the association of hydrological variables with large scale atmospheric/oceanic oscillations from different parts of the world. For the investigation of hydroclimatic teleconnections, first, the rainfall series and different climate oscillation series are decomposed individually by the traditional EMD approach. Here, the rainfall, QBO, and AMO resulted in six modes, while the ENSO and EQUINOO resulted in seven modes. Thus, mode misalignment exists between rainfall and ENSO (or EQUINOO), which may be due to the improper distribution of frequencies among different modes. It may eventually lead to the display of spurious associations and misinterpretations while performing a running correlation analysis. Therefore, all the five signals are decomposed simultaneously by employing MEMD. For this letter, the number of directions is selected as 64, and the tolerance and splitting parameters are selected as 0.075, 0.75, and 0.075, following the suggestions made in the past works [17], [23] to perform the MEMD of the multivariate data set. MEMD resulted in seven modes and residue for all the time series. The mean periods of the different modes computed by the zero-crossing method [16] are given in Table I.

The TDIC plots resulting from such associations of QBO, ENSO, EQUINOO, and AMO with rainfall time series are presented in Figs. 1–4, respectively. Fig. 1 depicts the association

TABLE I
Mean Period of Modes of Rainfall and Climate Oscillations (Expressed in Years) and the Average Period of Process Scale. LT Refers to the Long Term

Mode	Mean Period					Average
Number	Rainfall	QBO	ENSO	EQUINOO	AMO	Period
IMF1	1.1	1.0	1.1	1.0	1.1	1.0
IMF2	2.2	2.5	2.4	2.2	2.4	2.2
IMF3	4.0	3.4	4.2	3.7	4.0	3.7
IMF4	6.5	6.5	7.6	7.0	7.6	7.6
IMF5	14.0	14.0	14.0	12.0	10.5	16.8
IMF6	28.0	21.0	28.0	21.0	28.0	28.0
IMF7	84.0	84.0	84.0	84.0	42.0	42.0
Residue	LT	84.0	LT	84.0	LT	LT

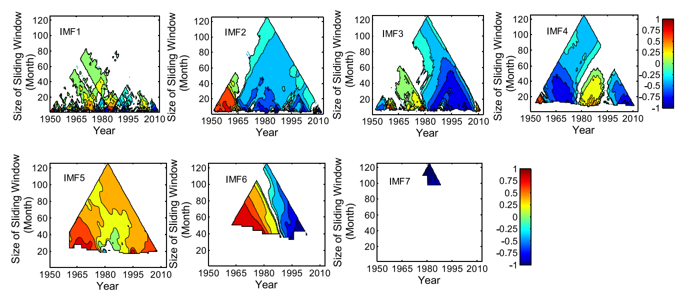

Fig. 1. TDIC plots between IMFs of QBO and summer monsoon rainfall in Kerala. The void spaces of the plot depict that correlation coefficients are not significant at 5% significance level.

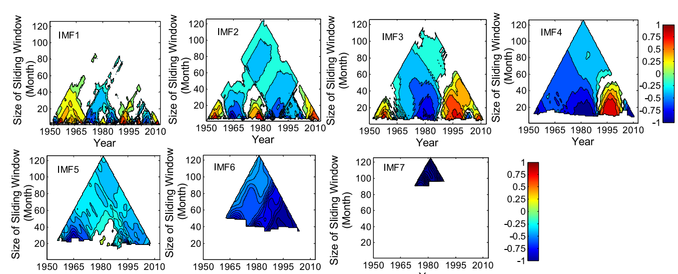

Fig. 2. TDIC plots between IMFs of ENSO and summer monsoon rainfall in Kerala. The void spaces of the plot depict that correlation coefficients are not significant at 5% significance level.

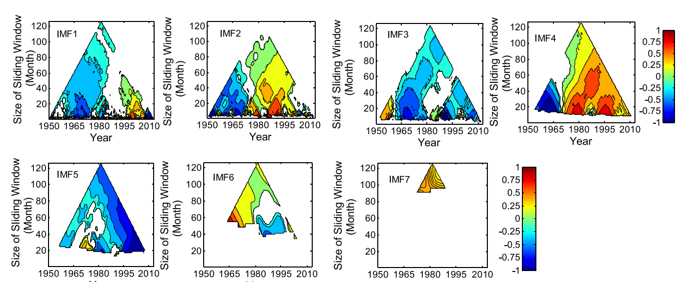

Fig. 3. TDIC plots between IMFs of EQUINOO and summer monsoon rainfall in Kerala. The void spaces of the plot depict that correlation coefficients are not significant at 5% significance level.

between QBO and summer monsoon rainfall in multiple time scales. A long range positive correlation between the respective IMFs is noticed in IMF5 (interdecadal), while the association is primarily negative in most of the other time scales. However, it is interesting to note a strong positive association between the

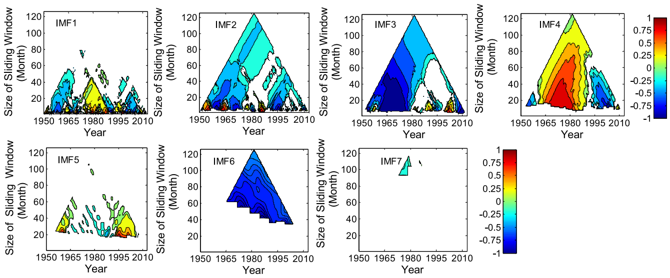

Fig. 4. TDIC plots between IMFs of AMO and summer monsoon rainfall in Kerala. The void spaces of the plot depict that correlation coefficients are not significant at 5% significance level.

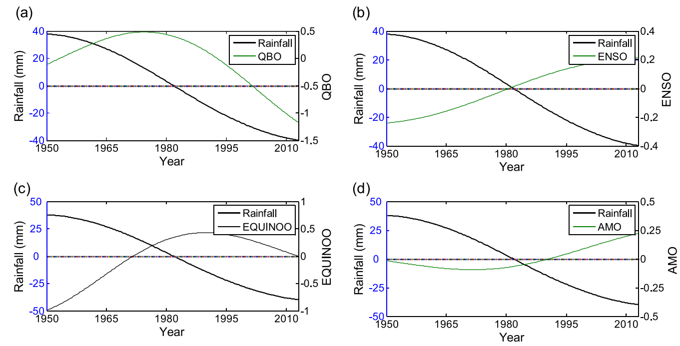

Fig. 5. Comparison of residue component of climate oscillation time series and rainfall time series. (a) QBO–rainfall. (b) ENSO–rainfall. (c) EQUINOO–rainfall. (d) AMO–rainfall.

TABLE II
CORRELATION COEFFICIENT (R) BETWEEN RAINFALL AND CLIMATIC OSCILLATIONS (CO) AT TWO LOW-FREQUENCY MODES (IMF7 AND RESIDUE)

Mode \ CO	Correlation (R) between rainfall and CO			
	QBO	ENSO	EQUINOO	AMO
IMF7	-0.914	-0.983	0.322	0.015
Residue	0.726	-0.998	-0.768	-0.834

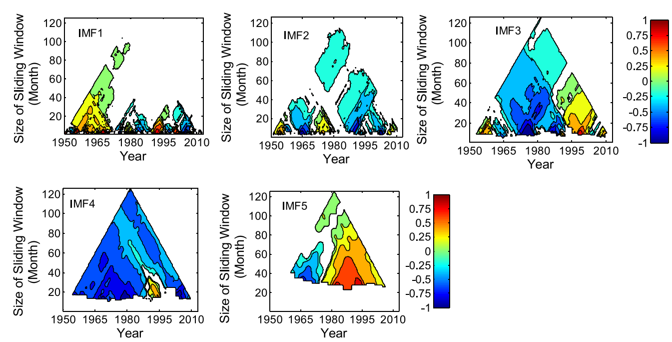

Fig. 6. TDIC plots between the IMFs of ENSO and summer monsoon rainfall in Kerala obtained by the EMD algorithm. The void spaces of the plot depict that correlation coefficients are not significant at 5% significance level.

time series in shorter time spells (for example, prior to 1965 in IMF3 and 1965–1980 in IMF6).

In the ENSO–rainfall link, a dominancy of negative association is noticed with the exception of positive associations in interdecadal scales of four years and seven years (IMF3 and IMF4) during 1995–2000. In the EQUINOO–rainfall link, a dominancy of negative association is noticed in IMF1, IMF3, and IMF5, and strong positive association exists in mode 4, while weak positive association exists in mode 2 and mode 6.

In the AMO–rainfall link, the association is negative in IMFs 2, 3, and 6, while the association is weak and is significant in IMF1 and IMF5. Here, a strong positive association is noticed between the two in IMF4 with a switchover to negative association since 1995 in the short–medium time spell ranges.

In general, the following points are noticed: 1) There are many reversals in the nature of association (switching to positive correlation from negative and vice versa) between the two series in the time domain in different process scales. Even though an exact reason behind such "switchovers" cannot be adduced from the obtained results, it helps to draw some broad inferences. The changes in local weather systems, influence of cyclonic events, etc., may be the reason behind such switchovers, as they modulate the rainfall processes in the region. 2) The reversals are more frequent in the high frequency mode (IMF1). 3) The strength of association (discerned by the color scheme of different TDIC plots) was also found to be varying over the time scale and with time spells. By capturing such information, it is possible to omit the less contributing (less significant) components at different time scales, which subsequently may improve the predictive capabilities of rainfall.

From Figs. 1–4, it is observed that, with the increase in mode number, an upward shift occurs in TDIC plots. Hence, in IMF7, significant correlation was noticed only for longer time spells close to or exceeding half the data length. To assess the association between rainfall and climate oscillations at such low-frequency modes, the correlation of modes are computed for IMF7 and residue. The results are presented in Table II. Similarly, to understand the nature of the evolution of the long-term trend, the zero-mean residue of rainfall is compared with that of different climate oscillations. These results are presented in Fig. 5.

Table II shows that, in the ENSO–rainfall link, the correlation is high and negative in both of the low-frequency time scales. Fig. 5 also shows that the association is purely negative for the ENSO–rainfall link, and here, the evolution is similar (as the zero crossing occurs nearly at the same time instant in the 1980s). In QBO, a fairly positive association can be noticed over the entire time span, while for the remaining two oscillations, the long-term nonlinear trend is showing no direct pattern. Also, the evolution of the trend is different as the zero crossing occurs at different time instants for different oscillations.

V. DISCUSSION

To examine the efficacy of the proposed MEMD–TDIC approach for teleconnection studies, the most debated ENSO–rainfall link [2], [3] is considered. The TDIC plots between the first five IMFs obtained by the individual decomposition (by EMD) of ENSO and rainfall are presented in Fig. 6. A careful perusal of Figs. 2 and 6 shows that, in Fig. 2, a strong positive association is displayed after 1995 for both IMF3 and IMF4, while it is completely lacking in IMF4 and rather weak in the IMF3 of Fig. 6. It may be noted that the process scales of these modes (4–7 years) fairly match with the periodicity of a typical El Niño event, and hence, the display of correlations in these modes needs special attention.

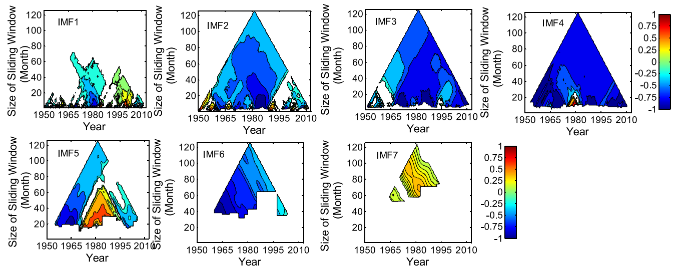

Fig. 7. TDIC plots between IMFs of ENSO and all India summer monsoon rainfall. The void spaces of the plot depict that correlation coefficients are not significant at 5% significance level.

Also, it is noted that, during 2002–2003, a strong negative correlation between the two is displayed in different modes in Fig. 2, while it is not observed in Fig. 6. Hence, it is inferred that such "true" associations are captured in a much better way by the proposed MEMD–TDIC approach for teleconnection studies, when compared with the EMD-based TDIC approach. To investigate the changes in such association at the local scale, the all India summer monsoon rainfall data are decomposed by MEMD (which resulted in eight modes), and the TDIC analysis is performed with the four climate indices. The result of the ENSO–rainfall link is presented in Fig. 7. The plot displays the well-debated negative association between the two in different time scales, and the pattern is quite different from that obtained for Kerala (see Fig. 2), which also shows the importance of hydroclimatic teleconnection studies at local scales.

The scale separation by MEMD is purely data adaptive. Hence, it eliminates the necessity of selection of the appropriate basis function (like mother wavelets or trigonometric functions). However, the theory of MEMD is more empirical in nature, and the control parameters should be fixed in such a way that, during the "automatic" scale separation, it should not result in overdecomposition. MEMD identifies common time scales in a multivariate data set; hence, it ensures the same number of modes for all variables and maintains "mode alignment." Hence, it is capable to decipher the "true" associations in teleconnection studies. The TDIC method solves the problem of random fixation of the sliding window size. It avoids the selection of the appropriate mother wavelet function and subsequent smoothing, which is necessary in a similar technique, wavelet coherence [24], [25].

VI. Conclusion

This letter proposed the MEMD–TDIC coupled approach for hydroclimatic teleconnection studies in India. It investigated the teleconnections of the summer monsoon rainfall in the coastal state of the Kerala state in India with four global climatic oscillations. The correlation patterns displayed by the TDIC plots in multiple time scales showed that the hydroclimatic teleconnections vary both in process scale and time domain and there may be multiple reversals in the strength and nature of their associations. The comparison of TDIC plots of the ENSO–rainfall link by the MEMD–TDIC approach with that by EMD–TDIC showed that the former approach captured the positive association between the two in 1997–1998 and the negative association during 2002–2003 clearly, owing to the mode alignment property of the MEMD method.

References

[1] G. Walker, "Correlation in seasonal variations of weather, VII: A preliminary study of world weather," *Memoirs India Meteorol. Dept.*, vol. 24, no. 4, pp. 75–131, 1923.

[2] K. B. Krishna Kumar, B. Rajagopalan, and M. A. Cane, "On the weakening relationship between the Indian monsoon and ENSO," *Science*, vol. 284, pp. 2156–2159, 1999.

[3] S. Gadgil, P. N. Vinayachandran, P. A. Francis, and S. Gadgil, "Extremes of the Indian summer monsoon rainfall, ENSO and equatorial Indian Ocean oscillation," *Geophys. Res. Lett.*, vol. 31, 2004, Art. no. L12213, doi: 10.1029/2004GL019733.

[4] C. Claud and T. Pascal, "Revisiting the possible links between the quasi-biennial oscillation and the Indian summer monsoon using NCEP R-2 and CMAP fields," *J. Clim.*, vol. 20, pp. 773–787, 2007.

[5] B. N. Goswami, M. S. Madhusoodanan, C. P. Neema, and S. Sengupta, "A physical mechanism for North Atlantic SST influence on the Indian summer monsoon," *Geophys. Res. Lett.*, vol. 33, 2006, Art. no. L02706, doi: 10.1029/2005GL024803.

[6] R. P. Kane, "Extremes of the ENSO phenomenon and Indian summer monsoon rainfall," *Int. J. Climatol.*, vol. 18, pp. 775–791, 1998.

[7] R. Maity and D. N. Kumar, "Hydroclimatic teleconnection between global sea surface temperature and rainfall over India at subdivisional monthly scale," *Hydrol. Process.*, vol. 21, no. 14, pp. 1802–1813, 2007.

[8] S. S. Kashid, S. Ghosh, and R. Maity, "Streamflow prediction using multisite rainfall obtained from hydroclimatic teleconnection," *J. Hydrol.*, vol. 395, no. 1/2, pp. 23–38, 2010.

[9] M. Janga Reddy and S. Adarsh, "Time frequency characterization of sub-divisional scale seasonal rainfall in India using Hilbert Huang transform," *Stochastic Environ. Res. Risk Assess.*, vol. 30, no. 4, pp. 1063–1085, 2016.

[10] N. E. Huang *et al.*, "The empirical mode decomposition and the Hilbert spectrum for nonlinear and non-stationary time series analysis," *Proc. Roy. Soc. A, Math., Phys. Eng. Sci.*, vol. 454, no. 1971, pp. 903–995, Mar. 1998.

[11] X. Chen, Z. Wu, and N. E. Huang, "The time-dependent intrinsic correlation based on the empirical mode decomposition," *Adv. Adapt. Data Anal.*, vol. 2, pp. 233–265, 2010.

[12] Y. Huang and F. G. Schmitt, "Time dependent intrinsic correlation analysis of temperature and dissolved oxygen time series using empirical mode decomposition," *J. Marine Syst.*, vol. 130, pp. 90–100, 2014.

[13] D. K. B. Ismail, P. Lazure, and I. Puillat, "Advanced spectral analysis and cross correlation based on empirical mode decomposition: Application to the environmental time series," *IEEE Geosci. Remote Sens. Lett.*, vol. 12, no. 9, pp. 1968–1972, Sep. 2015.

[14] N. Rehman and D. P. Mandic, "Multivariate empirical mode decomposition," *Proc. Roy. Soc. A*, vol. 466, no. 2117, pp. 1291–1302, 2010.

[15] G. Huang, Y. Su, A. Kareem, and H. Liao, "Time-frequency analysis of non-stationary process based on multivariate empirical mode decomposition," *J. Eng. Mech.*, vol. 142, no. 1, 2016, doi: 10.1061/(ASCE)EM.1943-7889.0000975.

[16] N. E. Huang *et al.*, "On instantaneous frequency," *Adv. Adapt. Data Anal.*, vol. 1, no. 2, pp. 177–229, 2009.

[17] W. Hu and B. C. Si, "Soil water prediction based on its scale-specific control using multivariate empirical mode decomposition," *Geoderma*, vol. 193/194, pp. 180–188, Feb. 2013.

[18] N. E. Huang *et al.*, "A confidence limit for the empirical mode decomposition and Hilbert spectral analysis," *Proc. Roy. Soc. A Math., Phys. Eng. Sci.*, vol. 459, no. 2037, pp. 2317–2345, Sep. 2003.

[19] E. Bedrosian, "A product theorem for Hilbert transforms," *Proc. IEEE*, vol. 51, no. 5, pp. 868–869, May 1963.

[20] A. H. Nuttall, "On the quadrature approximation to the Hilbert transform of modulated signals," *Proc. IEEE*, vol. 54, no. 10, pp. 1458–1459, Oct. 1966.

[21] R. Maity and D. N. Kumar, "Bayesian dynamic modeling for monthly Indian summer monsoon rainfall using El Niño—Southern Oscillation (ENSO) and Equatorial Indian Ocean Oscillation (EQUINOO)," *J. Geophys. Res.*, vol. 111, 2006, Art. no. D07104, doi: 10.1029/2005JD006539.

[22] K. J. Thara, "Response of Eastern Arabian sea to extreme climatic events with special reference to selected pelagic fishes," Ph.D. dissertation, Dept. Phys. Ocean., School Marine Sci., Cochin Univ. Sci. Technol., Kochi, India, 2011.

[23] G. Rilling, P. Flandrin, and P. Goncalves, "On Empirical mode decomposition and its algorithms," in *Proc. IEEE-EURASIP Workshop Nonlinear Signal Image Process.*, 2003, vol. 3, pp. 8–11.

[24] C. Torrence and G. P. Compo, "A practical guide to wavelet analysis," *Bull. Amer. Meteorol. Soc.*, vol. 79, pp. 61–78, 1998.

[25] P. C. Liu, "Wavelet spectrum analysis and ocean wind waves," in *Wavelets in Geophysics*, E. Foufoula-Georgiou and P. Kumar, Eds. San Diego, CA, USA: Academic, 1994, pp. 151–166.